

Supporting Information

Improving external quantum efficiency and efficiency roll-off in OLEDs:
A study on donor linkage and acceptor nitrogen atom position
optimization in TADF emitters

Gyana Prakash Nanda, Rajan Suraksha, Bahadur SK, Thamodharan Viswanathan, and
Pachaiyappan Rajamalli*

Materials Research Centre, Indian Institute of science, Bangalore, Karnataka, 560012, India

Email: rajamalli@iisc.ac.in

Table

Sl No.	Content	Page no.
1.	Instrumentation	2
2.	Materials	2-3
3.	Synthesis	3-7
	3.1. Synthesis of 3BPy- <i>m</i> DPXZ	3-4
	3.2. Synthesis of 3BPy- <i>m</i> PXZ	4-5
	3.3. Synthesis of 3BPy- <i>p</i> PXZ	5-6
	3.4. Synthesis of 4BPy- <i>p</i> PXZ	6-7
4.	Thermogravimetric analysis (TGA)	7
5.	Electrochemical studies (CV)	8-9
6.	Theoretical calculations (TD-DFT)	9-11
7.	Photophysical studies	12
	7.1. UV-Visible absorption	12
	7.2. Film PL measurement	12
8.	Lifetime measurement	13-14

9.	Electroluminescence (EL) properties	15-17
10.	NMR spectra	18-25
11.	Reference	25

Instrumentation

¹H NMR and ¹³C NMR spectra were recorded from a Bruker Advance 400 MHz and 500 MHz spectrometers. High-resolution mass spectra (HRMS) spectra were obtained from MAT-95XL HRMS. UV-visible absorption spectra were taken in Hitachi U-3300 spectrophotometer. Fluorescence and phosphorescence spectra were recorded on a Hitachi F-7100 spectrophotometer. Excited state lifetimes were recorded in Quantaaurus-Tau (Hamamatsu Photonics). Thermal stability was studied using TA Instruments Q50 TGA thermogravimetric analyzer. The cyclic voltammetry measurements were done using BioLogic SP300 potentiostat (BioLogic, France). The ground state molecular geometries of the emitters were optimized employing time dependent density functional theory (TD-DFT) B3LYP hybrid functional and 6-311G (d, p) basis set in Gaussian 09 software using SERC facility @ IISc. Gauss View 5.0 was used to analyse the molecular orbitals.

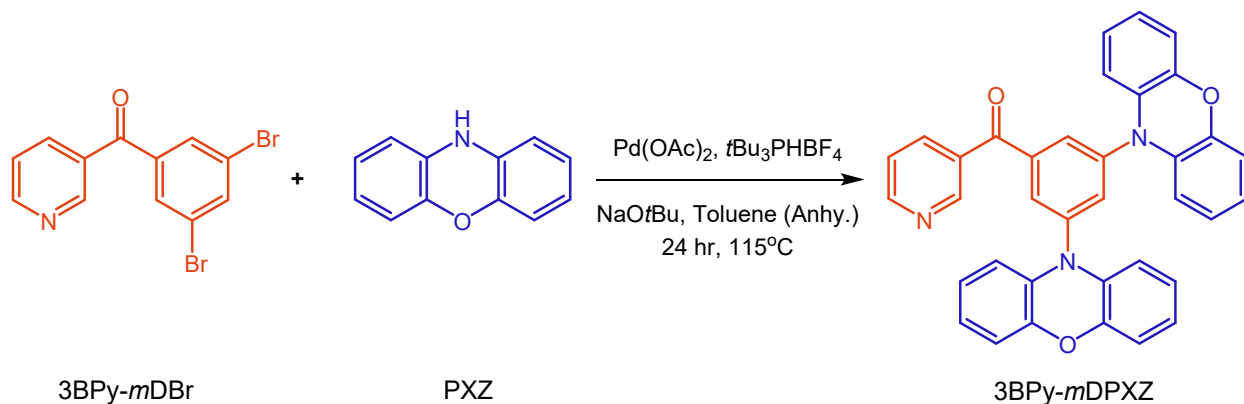
Materials

All the starting materials, reagents, and catalysts for emitter synthesis were commercially purchased from BLD pharma (India) PVT. LTD., and were used without further purification. Materials for OLED device fabrications were also commercially purchased from BLD pharma (India) PVT. LTD., and were purified by vacuum sublimation before used in the device. NMR

solvents (CDCl_3) was commercially purchased from SYNMR CHEMICALS PVT. LTD. Bangalore.

Synthesis

Synthesis of (3,5-di(10*H*-phenoxazin-10-yl)phenyl)(pyridin-3-yl)methanone (3BPY-*m*DPXZ)

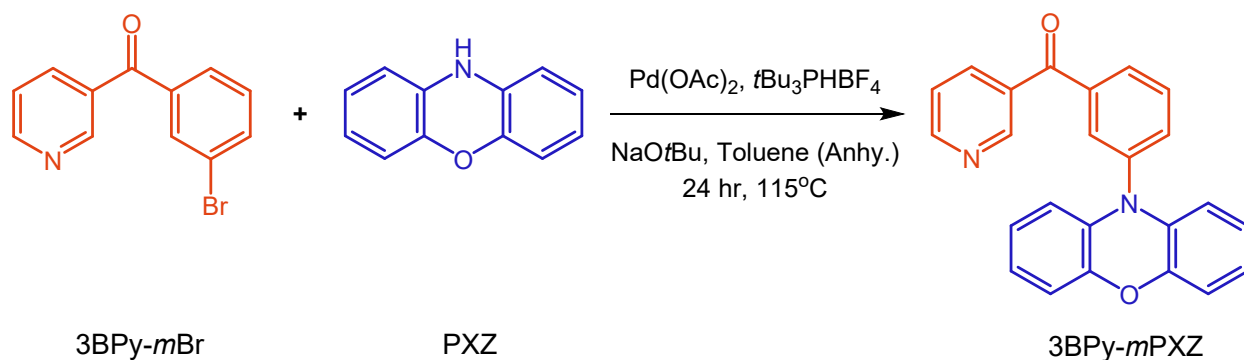


Scheme S1. Molecular structure and synthesis route of 3BPY-*m*DPXZ.

In a 100 ml cleaned and dried sealed tube, (3,5-dibromophenyl)(pyridin-3-yl)methanone (3BPY-*m*DBr) (1 g, 2.9 mmol), 10*H*-phenoxazine (PXZ) (1.18 g, 6.4 mmol), palladium acetate (0.065 g, 10 mol%), tri-*tert*-butyl phosphine tetrafluoro borate (0.13 g, 0.44 mmol), and sodium *tert*-butoxide (0.7 g, 7.3 mmol) were taken.¹ After evacuating air, the sealed tube was purged with nitrogen and the process was repeated for three times. Under nitrogen condition, the solid mixture was dissolved in 40 ml of anhydrous toluene and then allowed the reaction mixture to stir at 115 °C for 24 hours. The progress of the reaction was checked through TLC. After completion of the reaction, toluene was removed under reduced pressure and product was extracted with ethyl acetate. The final organic part was concentrated under reduced pressure. The compound was purified by silica gel column chromatography using ethyl-acetate/ *n*-hexane as eluent to afford yellow coloured (3,5-di(10*H*-phenoxazin-10-yl)phenyl)(pyridin-3-yl)methanone (3BPY-*m*DPXZ)

with 50% yield. $^1\text{H NMR}$ (400 MHz, Chloroform- d) δ 9.03 (s, 1H), 8.82 (s, 1H), 8.17 (d, $J = 7.4$ Hz, 1H), 7.92 (d, $J = 1.9$ Hz, 2H), 7.72 (s, 1H), 7.48 (dd, $J = 7.9, 4.7$ Hz, 1H), 6.70 (dd, $J = 4.7, 1.9$ Hz, 8H), 6.67 (dd, $J = 7.1, 3.2$ Hz, 4H), 6.07 – 5.96 (m, 3H). $^{13}\text{C NMR}$ (101 MHz, Chloroform- d) δ 192.43, 153.54, 150.76, 144.09, 142.69, 142.30, 139.00, 137.10, 133.47, 132.55, 132.23, 123.73, 123.47, 122.34, 116.09, 113.13. HRMS (ESI+) calcd for $\text{C}_{36}\text{H}_{24}\text{N}_3\text{O}_3$ $[\text{M} + \text{H}]^+$, 546.1817 and found 546.1805.

Synthesis of (3-(10H-phenoxazin-10-yl)phenyl)(pyridin-3-yl)methanone (3BPy-*m*PXZ)

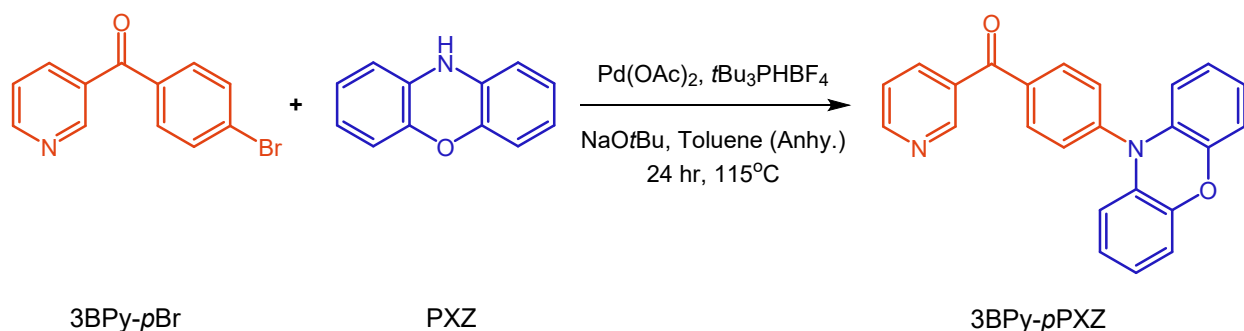


*Scheme S2. Molecular structure and synthesis route of 3BPy-*m*PXZ.*

In a 100 ml cleaned and dried sealed tube, (3-bromophenyl)(pyridin-3-yl)methanone (3BPy-*m*Br) (1 g, 3.8 mmol), 10H-phenoxazine (PXZ) (0.74 g, 4.0 mmol), palladium acetate (0.086 g, 10 mol%), tri-*tert*-butyl phosphine tetrafluoro borate (0.17 g, 0.57 mmol), and sodium *tert*-butoxide (0.55 g, 5.7 mmol) were taken.² After evacuating air, the sealed tube was purged with nitrogen and this process was repeated three times. Then 40 ml of anhydrous toluene was added, and the reaction mixture was allowed to stir at 115 °C for 24 hours. After completion of the reaction, toluene was removed under reduced pressure and product was extracted with ethyl acetate. The final organic part was concentrated under reduced pressure. The compound was purified by silica gel column chromatography using ethyl-acetate/ *n*-hexane as eluent to afford yellow coloured (3-(10H-

phenoxazin-10-yl)phenyl)(pyridin-3-yl)methanone (3BPY-*m*PXZ) with 50% yield. ¹H NMR (400 MHz, Chloroform-*d*) δ 8.98 (d, *J* = 2.2 Hz, 1H), 8.79 (dd, *J* = 4.9, 1.8 Hz, 1H), 8.11 (dt, *J* = 8.0, 2.0 Hz, 1H), 7.92 (dt, *J* = 7.7, 1.5 Hz, 1H), 7.79 (t, *J* = 1.9 Hz, 1H), 7.74 (t, *J* = 7.7 Hz, 1H), 7.63 (dt, *J* = 7.9, 1.5 Hz, 1H), 7.43 (ddd, *J* = 7.9, 4.9, 1.0 Hz, 1H), 6.68 (dd, *J* = 7.7, 2.0 Hz, 2H), 6.64 (td, *J* = 7.5, 1.6 Hz, 2H), 6.59 (td, *J* = 7.5, 2.0 Hz, 2H), 5.90 (dd, *J* = 7.8, 1.6 Hz, 2H). ¹³C NMR (101 MHz, Chloroform-*d*) δ 193.60, 154.07, 153.23, 150.87, 143.94, 139.77, 139.65, 137.15, 136.14, 133.91, 132.68, 132.64, 131.62, 129.96, 123.57, 121.85, 115.74, 113.13. HRMS (ESI+) calcd for C₂₄H₁₇N₂O₂ [M + H]⁺, 365.1290 and found 365.1286.

Synthesis of (3-(10*H*-phenoxazin-10-yl)phenyl)(pyridin-3-yl)methanone (3BPY-*p*PXZ)

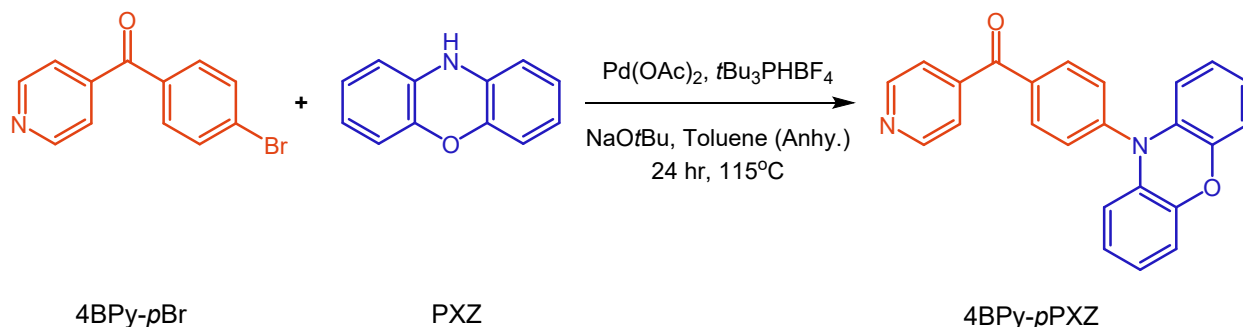


Scheme S3. Molecular structure and synthesis route of 3BPY-*p*PXZ.

In a 100 ml cleaned and dried sealed tube, (3-bromophenyl)(pyridin-3-yl)methanone (3BPY-*p*Br) (1 g, 3.8 mmol), 10*H*-phenoxazine (PXZ) (0.74 g, 4.0 mmol), palladium acetate (0.086 g, 10 mol%), tri-*tert*-butyl phosphine tetrafluoro borate (0.17 g, 0.57 mmol), and sodium *tert*-butoxide (0.55 g, 5.7 mmol) were taken. After evacuating air, the sealed tube was purged with nitrogen and this process was repeated three times. Then 40 ml of anhydrous toluene was added, and the reaction mixture was allowed to stir at 115 °C for 24 hours. After completion of the reaction, toluene was removed under reduced pressure and product was extracted with ethyl acetate. The final organic

part was concentrated under reduced pressure. The compound was purified by silica gel column chromatography using ethyl-acetate/ *n*-hexane as eluent to afford yellow coloured (3-(10*H*-phenoxazin-10-yl)phenyl)(pyridin-3-yl)methanone (3BPy-*m*PXZ) with 50% yield. ¹H NMR (400 MHz, Chloroform-*d*) δ 9.03 (d, *J* = 1.3 Hz, 1H), 8.82 (d, *J* = 3.1 Hz, 1H), 8.16 (d, *J* = 8.4 Hz, 1H), 8.02 (d, *J* = 8.4 Hz, 2H), 7.50 (d, *J* = 8.4 Hz, 2H), 7.48 – 7.45 (m, 1H), 6.73 – 6.64 (m, 4H), 6.63 – 6.57 (m, 2H), 5.98 (d, *J* = 7.9 Hz, 2H). ¹³C NMR (101 MHz, Chloroform-*d*) δ 193.82, 153.18, 150.92, 144.10, 143.90, 137.13, 136.43, 133.60, 132.86, 132.72, 131.06, 123.53, 123.34, 122.03, 115.82, 113.44. HRMS (ESI+) calcd for C₂₄H₁₇N₂O₂ [M + H]⁺, 365.1290 and found 365.1288.

Synthesis of (4-(10*H*-phenoxazin-10-yl)phenyl)(pyridin-4-yl)methanone (4BPy-*p*PXZ)



Scheme S4. Molecular structure and synthesis route of 4BPy-*p*PXZ.

In a 100 ml cleaned and dried sealed tube, (4-bromophenyl)(pyridin-4-yl)methanone (4BPy-*p*Br) (1 g, 3.8 mmol), 10*H*-phenoxazine (PXZ) (0.74 g, 4.0 mmol), palladium acetate (0.086 g, 10 mol%), tri-*tert*-butyl phosphine tetrafluoro borate (0.17 g, 0.57 mmol), and sodium *tert*-butoxide (0.55 g, 5.7 mmol) were taken. After evacuating air, the sealed tube was purged with nitrogen and this process was repeated three times. Then 40 ml of anhydrous toluene was added, and the reaction mixture was allowed to stir at 115 °C for 24 hours. After completion of the reaction, toluene was removed under reduced pressure and product was extracted with ethyl acetate. The final organic

part was concentrated under reduced pressure. The compound was purified by silica gel column chromatography using ethyl-acetate/ *n*-hexane as eluent to afford yellow coloured (4-(10*H*-phenoxazin-10-yl)phenyl)(pyridin-4-yl)methanone (4BPy-*p*PXZ) with 50% yield. ¹H NMR (400 MHz, Chloroform-*d*) δ 8.83 (d, *J* = 6.0 Hz, 2H), 8.02 (d, *J* = 8.5 Hz, 2H), 7.62 (d, *J* = 6.0 Hz, 2H), 7.50 (d, *J* = 8.4 Hz, 2H), 6.77 – 6.64 (m, 4H), 6.63 – 6.56 (m, 4H), 5.98 (d, *J* = 7.9 Hz, 4H). ¹³C NMR (101 MHz, Chloroform-*d*) δ 194.05, 150.56, 144.34, 144.16, 143.98, 135.50, 133.53, 132.86, 131.01, 123.33, 122.77, 122.12, 115.88, 113.50. HRMS (ESI+) calcd for C₂₄H₁₇N₂O₂ [M + H]⁺, 365.1290 and found 365.1289.

Thermogravimetric analysis (TGA)

Thermal stabilities of the emitters were measured through thermogravimetric analysis (TGA) recorded under inert condition. At 5% weight loss, the degradation temperatures were measured shown in Figure S1.

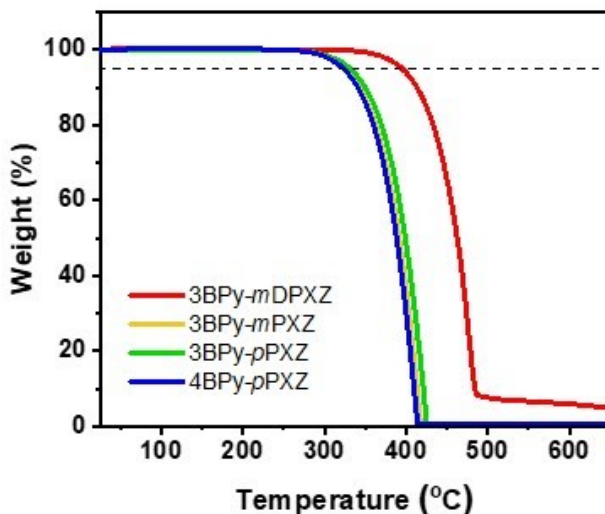


Figure S1. Thermogravimetric analysis of 3BPy-*m*DPXZ, 3BPy-*m*PXZ, 3BPy-*p*PXZ, and 4BPy-*p*PXZ measured under inert atmosphere. Decomposition temperature (*T_d*) measured at 5 % loss of the compounds.

Electrochemical properties

Electrochemical properties of the emitters were explored through cyclic voltametric (CV) measurements using three electrode system. CV was recorded for 1mM solution of emitters in degassed dichloromethane solution using Tetrabutylammonium hexafluorophosphate (TBAPF₆) as electrolyte, glassy carbon as working electrode, platinum as counter electrode, and Ag/ AgCl as standard reference electrode (Figure S2). As the CV curves are completely reversible, HOMO energy levels were evaluated from the half-wave potential of the emitter using the equation $E_{\text{HOMO}} = - [(E_{1/2} (\text{emitter}) - E_{1/2} (\text{ferrocene})) + 4.8]$ instead of oxidation onset. The LUMO energy levels were calculated from the formula $E_{\text{LUMO}} = E_{\text{HOMO}} - E_g$; where, E_g is the optical band gap of the emitter measured from onset of absorption plot.³ HOMO and LUMO energy level of 4BPY-pPXZ were measured to be -5.22 and -2.68 eV, respectively.

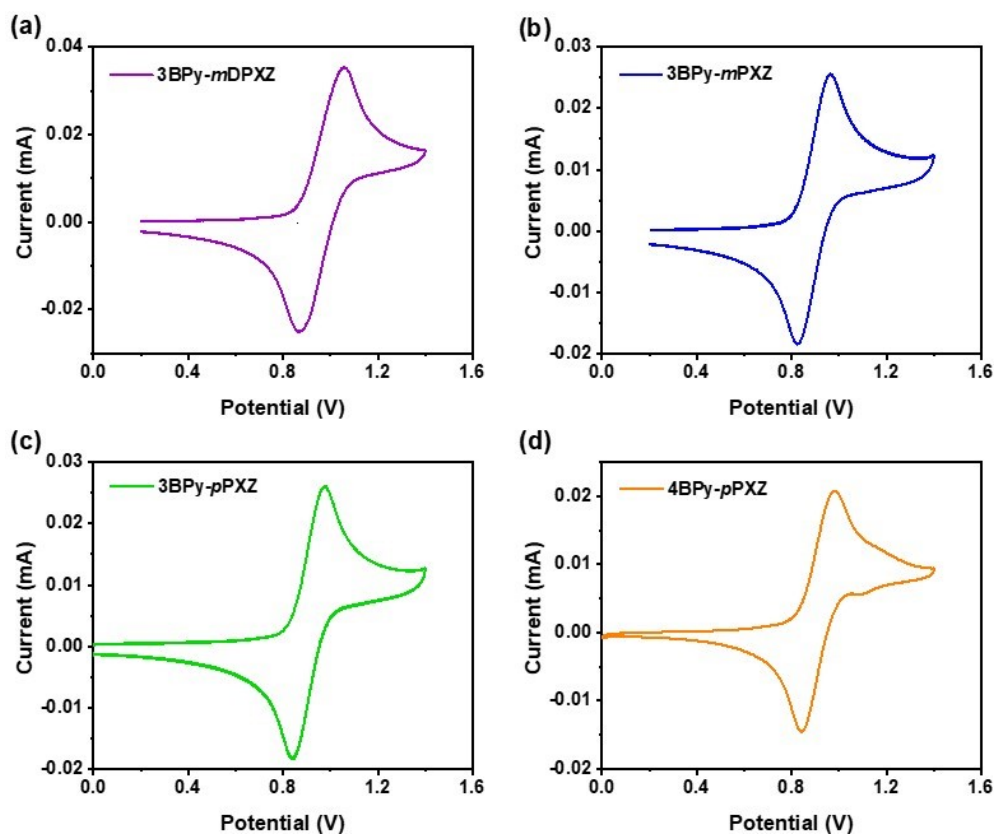


Figure S2. Cyclic voltammogram of (a) 3BPY-mDPXZ; (b) 3BPY-mPXZ; (c) 3BPY-pPXZ; (d) 4BPY-pPXZ recorded in degassed dichloromethane solvent using Tetrabutylammonium hexafluorophosphate (TBAPF₆)

as electrolyte, glassy carbon as working electrode, platinum as counter electrode, and Ag/AgCl as standard reference electrode.

Theoretical calculations (TD-DFT)

Time-dependent density functional theory (TD-DFT) calculations were performed using B3LYP/6-31g (d, p) basis sets to obtain an idea about the excited state energy levels of the emitters and the distribution of frontier molecular orbitals over the emitter molecules.⁴

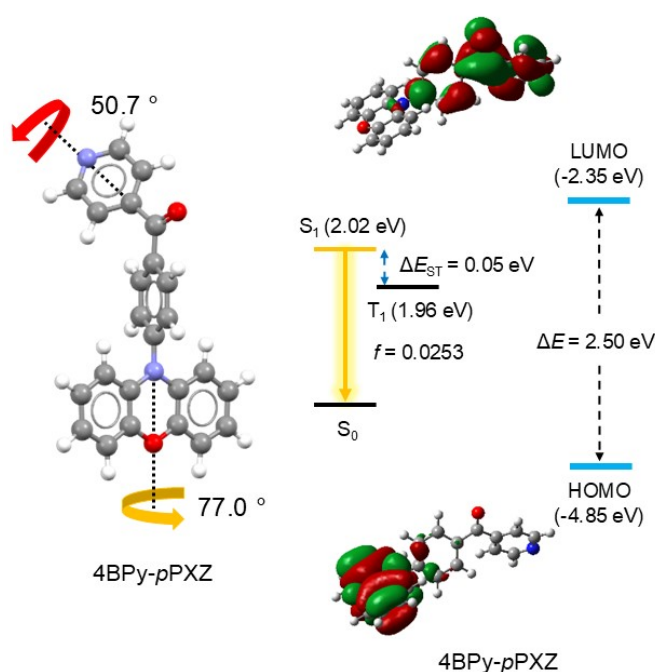


Figure S3. Optimized molecular structure of 4BPY-pPXZ showing the dihedral angles and the distribution of highest occupied molecular orbital and lowest unoccupied molecular orbital along with excited state energy level of the emitter.

The UV-Visible absorption spectra of the emitters obtained from the TD-DFT calculations are shown in Figure S4. A broad absorption band at high wavelength (low energy) region most probably corresponds to the intramolecular donor to acceptor charge transfer (ICT) transition.⁵ Among the four molecules the para donor derivatives have a significant intensity of the ICT band.

By changing the donor position to meta, the ICT band intensity is gradually decreasing. The energy levels of the emitters calculated from TD-DFT are shown in Table S1.

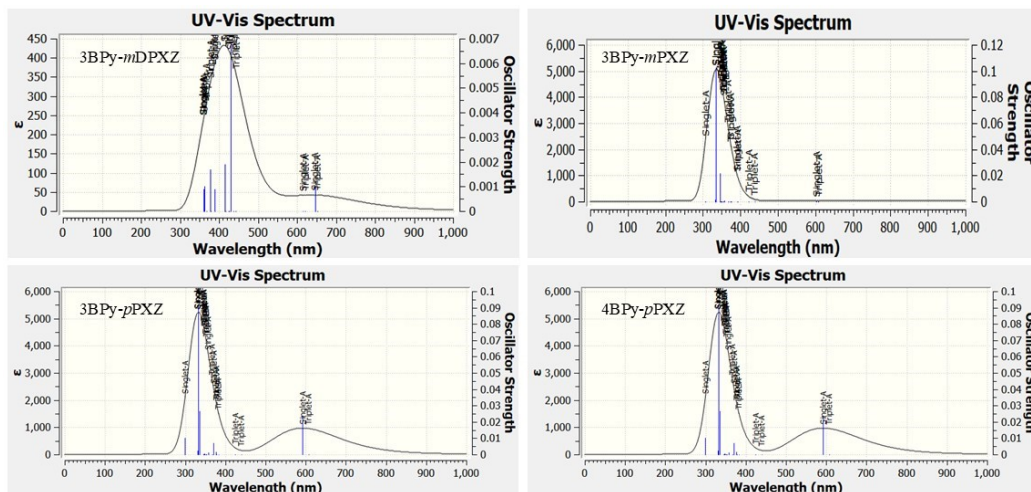


Figure S4. The UV-Visible absorption spectra of 3BPY-mDPXZ, 3BPY-mPXZ, 3BPY-pPXZ, and 4BPY-pPXZ obtained from TD-DFT calculations.

Optimized molecular structure of the emitters obtained from DFT calculations are shown in Figure S5. The dihedral angle between the phenoxazine donor and bridging phenyl group is comparatively larger in 3BPY-mDPXZ and 3BPY-mPXZ than 3BPY-pPXZ and 4BPY-pPXZ.

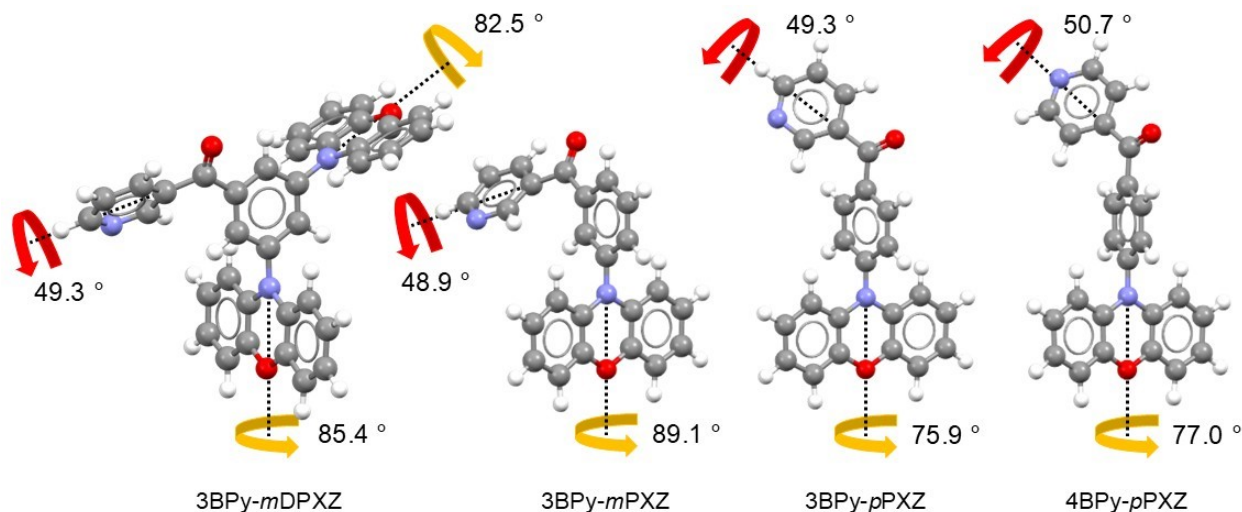


Figure S5. The optimized molecular structures of 3BPy-*m*DPXZ, 3BPy-*m*PXZ, 3BPy-*p*PXZ, and 4BPy-*p*PXZ obtained from DFT calculation showing the dihedral angle between donor unit and bridging phenyl group.

Table S1. Data obtained from TD-DFT calculations

Emitter	HOMO (eV)	LUMO (eV)	E_g (eV)	S_1 (eV)	T_1 (eV)	ΔE_{ST} (eV)	f
3BPy- <i>m</i> DPXZ	-4.81	-2.37	2.44	1.92	1.90	0.016	0.0010
3BPy- <i>m</i> PXZ	-4.76	-2.19	2.57	2.05	2.04	0.016	0.0005
3BPy- <i>p</i> PXZ	-4.79	-2.21	2.58	2.09	2.04	0.049	0.0237
4BPy- <i>p</i> PXZ	-4.85	-2.35	2.50	2.02	1.96	0.048	0.0253

HOMO: highest occupied molecular orbital; *LUMO*: lowest unoccupied molecular orbital; E_g : optical band gap; S_1 : singlet excited state energy; T_1 : triplet excited energy; ΔE_{ST} : singlet-triplet energy gap; f : oscillator strength.

Photophysical properties

UV-Visible absorption spectrum of 4BPy-*p*PXZ was recorded in toluene solution at 0.01 mM concentration (Figure S6). Emitter showing two broad absorption band, the absorption band at low energy region corresponds to donor to acceptor charge transfer transition.

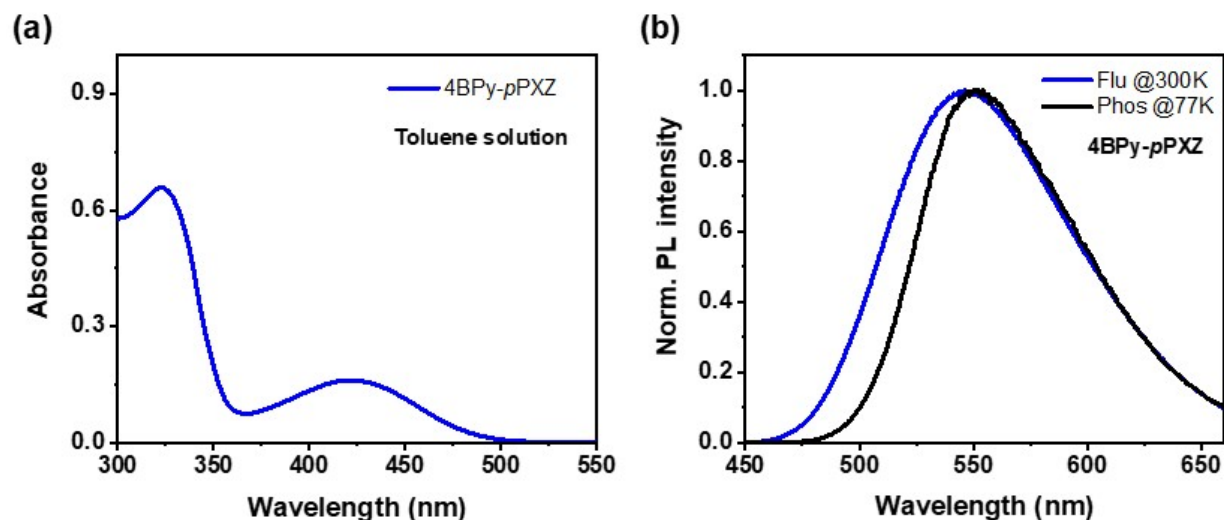


Figure S6. (a) UV-Visible absorption plot of 4BPY-pPXZ in toluene solution; (b) Room temperature fluorescence and low temperature phosphorescence spectra of 4BPY-pPXZ in their CBP host doped film.

Table S2. PL properties of 4BPY-pPXZ in CBP host doped film

Emitter	λ_{abs}^a (nm)	PL_{max}^b (nm)	S_1^c (eV)	T_1^d (eV)	ΔE_{ST}^e (eV)
4BPY-pPXZ	322, 422	547	2.61	2.49	0.11

a: Absorption maxima of 4BPY-pPXZ in 0.01 mM toluene solution; *b:* Emission maxima of emitters in CBP host doped film excited @ 340 nm; *c:* Singlet excited state energy levels of the emitters in the CBP doped film; *d:* Triplet excited state energy levels of the emitters in the CBP doped film; *e:* Singlet-triplet energy gap of the emitter.

Excited state lifetime measurement

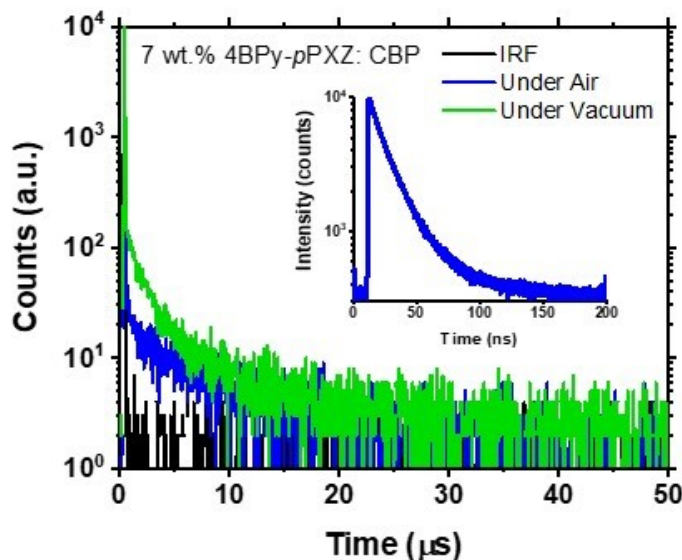


Figure S7. Excited state lifetimes of 4BPy-pPXZ in CBP host doped films recorded under ambient condition and under vacuum. [inserted prompt fluorescence lifetime of the emitter]

The solid-state photoluminescence measurements of 3BPy-mDPXZ, 3BPy-mPXZ, 3BPy-pPXZ, and 4BPy-pPXZ were performed in 7 wt.% emitter: CBP host matrix using excitation wavelength of 340 nm. All the emitters show structureless broad emission spectra in yellow-green region. The solid-state photoluminescence quantum yields (PLQYs) of the emitters in their CBP doped films were measured in an integrating sphere set up. Excited state lifetimes of the CBP doped films were measured under both inert and air condition. The kinetic parameters and PLQY values are summarized in Table S3.

Table S3. Transient PL measurement of the emitters in CBP host doped films

Parameters	3BPy-mDPXZ	3BPy-mPXZ	3BPy-pPXZ	4BPy-pPXZ
Φ_T (%)	8.99	18.12	73.85	63.61
Φ_P (%)	6.39	12.78	56.08	42.72
Φ_D (%)	2.6	5.34	17.77	20.89

τ_p (ns)	30.52	54.36	23.03	21.78
τ_D (us)	2.30	8.46	2.03	2.74
$k_p(R)$ [s^{-1}]	0.21×10^7	0.23×10^7	2.43×10^7	1.96×10^7
$k_p(T)$ [s^{-1}]	3.27×10^7	1.84×10^7	4.34×10^7	4.59×10^7
$k_D(T)$ [s^{-1}]	4.35×10^5	1.18×10^5	4.93×10^5	3.65×10^5
k_{ISC} [s^{-1}]	9.6×10^7	5.4×10^6	1.05×10^7	1.51×10^7
k_{RISC} [s^{-1}]	6.04×10^5	1.67×10^5	6.48×10^5	5.43×10^5

Φ_T : PLQY under vacuum; Φ_P : PLQY under air; Φ_D : PLQY difference; τ_p : prompt lifetime; τ_D : delayed lifetime; $k_p(R)$: Radiative prompt component; $k_p(T)$: Total prompt component; $k_D(T)$: Total delayed component; k_{ISC} : intersystem crossing rate constant; k_{RISC} : reverse intersystem crossing rate constant.

Below are the equations to calculate different kinetic parameters using the lifetime and PLQY values.¹

$$k_{ISC} = [\Phi_D \times k_p \text{ (total)}] / [\Phi_{PL}] \quad \dots\dots \text{(I)}$$

$$k_{RISC} = [k_D \text{ (total)} \times k_p \text{ (total)} \times \Phi_D] / [\Phi_P \times k_{ISC}] \quad \dots\dots \text{(II)}$$

$$k_{IC} = k_p \text{ (total)} - [k_p \text{ (radiative)} + k_{ISC}] \quad \dots\dots \text{(III)}$$

$$k_p \text{ (total)} = 1 / \tau_p \quad \dots\dots \text{(IV)}$$

$$k_p \text{ (radiative)} = \Phi_P / \tau_p \quad \dots\dots \text{(V)}$$

$$k_D \text{ (total)} = 1 / \tau_D \quad \dots\dots \text{(VI)}$$

Where,

Φ_P is the PLQY under air, Φ_T is the total PLQY, Φ_D is the difference between Φ_T and Φ_P , τ_p is the prompt lifetime, τ_D is the delayed lifetime,

Electroluminescence (EL) properties

Organic light emitting diode (OLED) fabrication details: Before fabrication the devices, the substrates were properly cleaned. Indium tin oxide (ITO) coated glass substrates were sonicated with detergent, hot DI water, and isopropanol for 10 minutes. The substrates were dried using nitrogen gun, and were then cleaned under ultraviolet ozone (UV-ozone) cleaner for 20 minutes. After ozone cleaning the substrates were loaded in to the vacuum chamber. Evaporation/ deposition was performed once the vacuum level reached 3×10^{-6} mbar. All the organic mater were deposited with an evaporation rate of 1 \AA/s . 8-Hydroxyquinolinolato-lithium (Liq) and aluminium were deposited with an evaporation rate of 0.1 \AA/s and $2-3 \text{ \AA/s}$, respectively.⁶ In the device architecture, N,N'-Di(1-naphthyl)-N,N'-diphenyl-(1,1'-biphenyl)-4,4'-diamine/ NPB was used as hole injection layer, 1,1-Bis[(di-4-tolylamino)phenyl]cyclohexane/ TAPC was used as hole transporting layer, Bis(N-carbazolyl)-1,1'-biphenyl/ CBP was used as host, 2,8-Bis(diphenylphosphoryl)-dibenzo[b,d]thiophene/ PPT was used as exciton/ hole blocking later, 2,2',2''-(1,3,5-Benzinetriyl)-tris(1-phenyl-1-H-benzimidazole)/ TPBi was used as electron transporting layer, 8-Hydroxyquinolinolato-lithium/ Liq was used as electron injection layer. Indian tin oxide/ ITO and aluminium/ Al were used as anode and cathode, respectively.⁶ Vacuum deposited OLED devices (D_1 to D_4) were fabricated using the newly synthesized emitter in the emissive layer (EML) doped with 4,4'-Bis(9-carbazolyl)-1,1'-biphenyl (CBP) host. In all devices EML has 7 weight % of emitters in CBP host.

Electroluminescence spectra of the devices showed no residual peaks even at higher voltages, suggesting the proper confinement of exciton recombination within the emissive layer, explaining the ideal design of device architecture (Figure S8).⁷

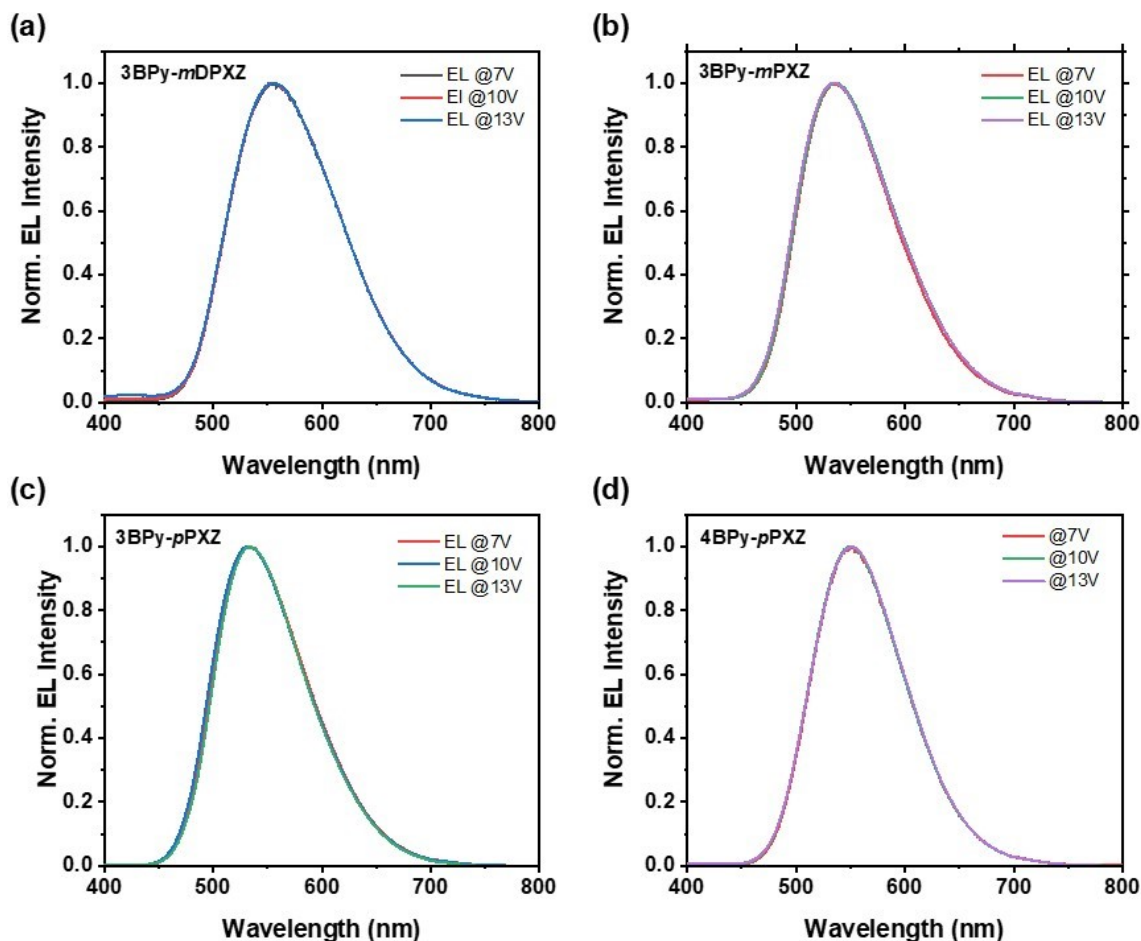


Figure S8. EL spectra of the OLED devices recorded at different voltages.

Power efficiency and current efficiency with respect to luminance plot of OLED devices incorporating CBP doped films of 3BPy-*m*DPXZ, 3BPy-*m*PXZ, 3BPy-*p*PXZ, and 4BPy-*p*PXZ are shown in Figure S9.

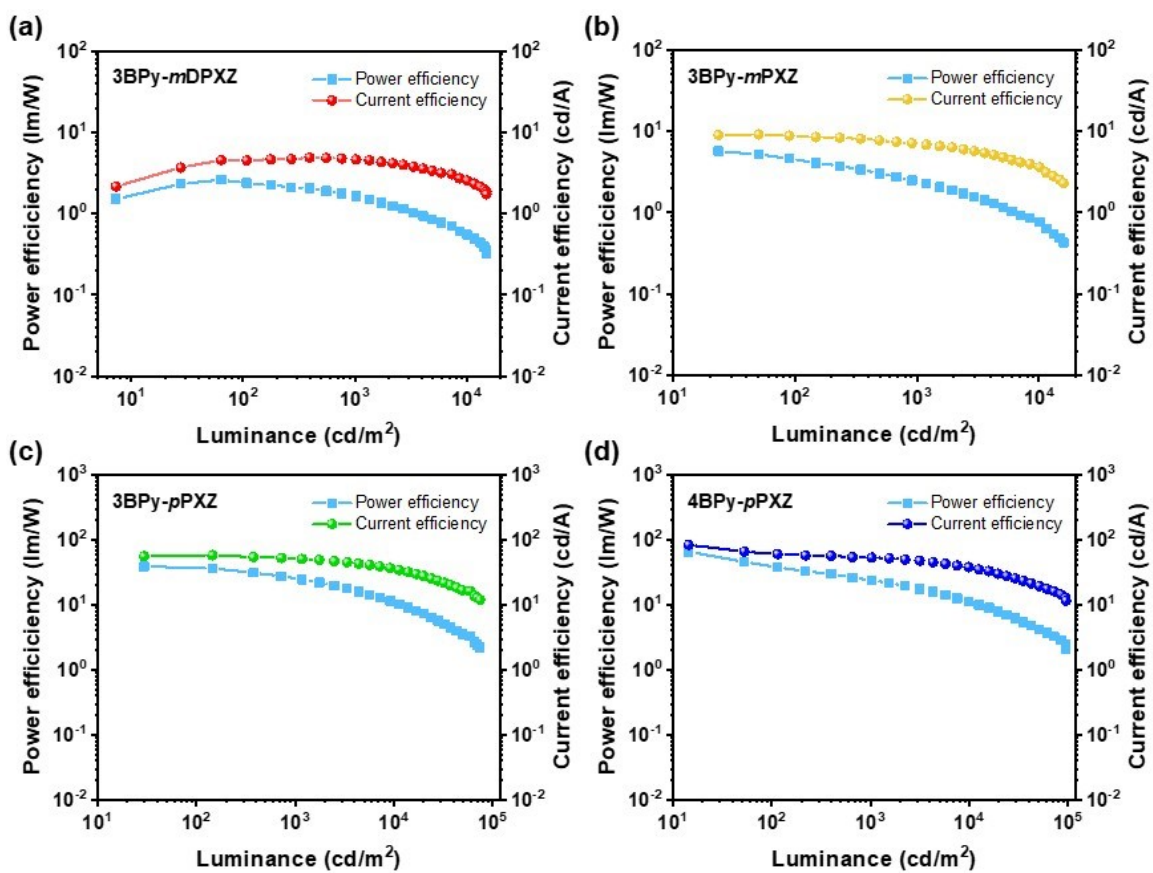


Figure S9. Power efficiency (lm/W) Vs Luminance (cd/m^2) Vs Current efficiency (cd/A) of (a) 3BPy-mDPXZ, (b) 3BPy-mPXZ, (c) 3BPy-pPXZ, and (d) 4BPy-pPXZ based OLED devices.

NMR spectra

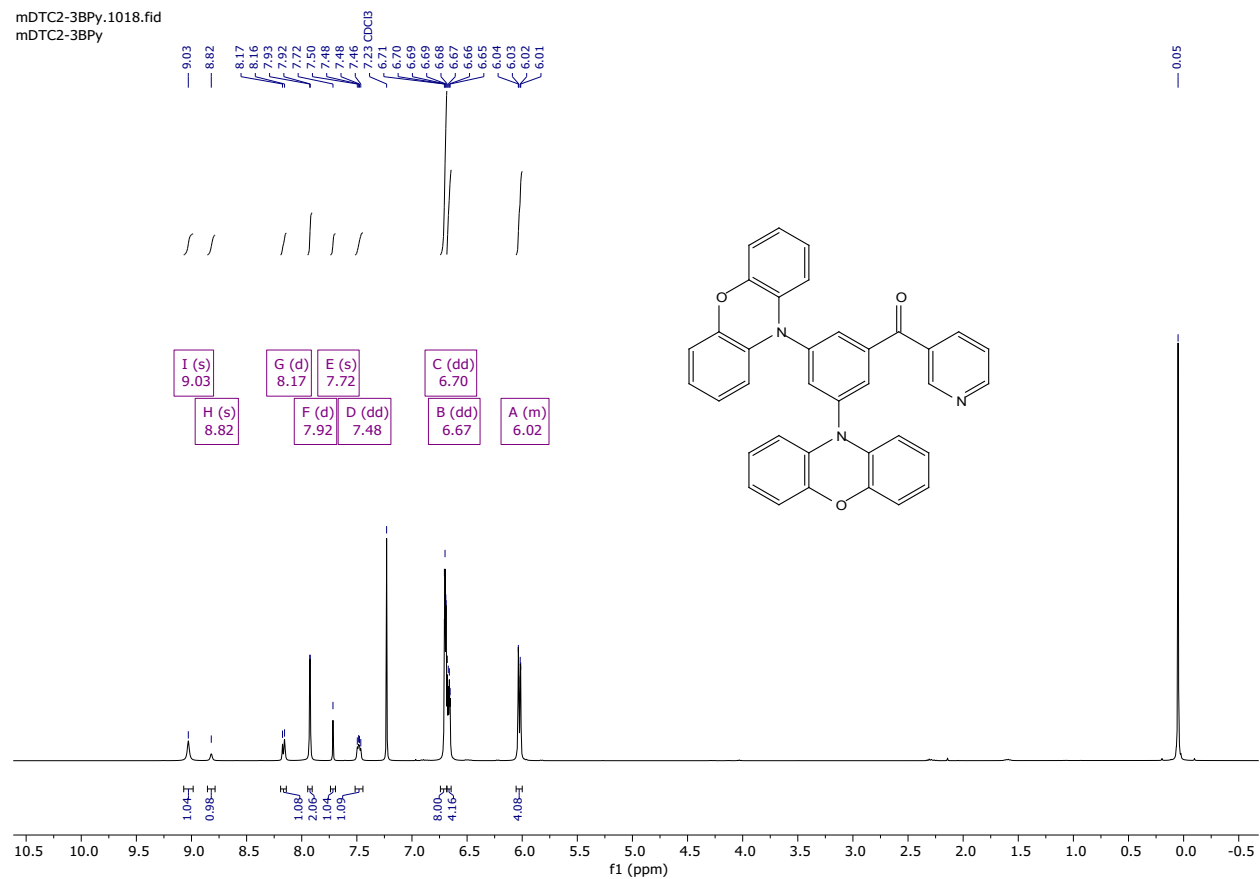


Figure S10. ^1H NMR of 3BPy-mDPXZ recorded in CDCl_3

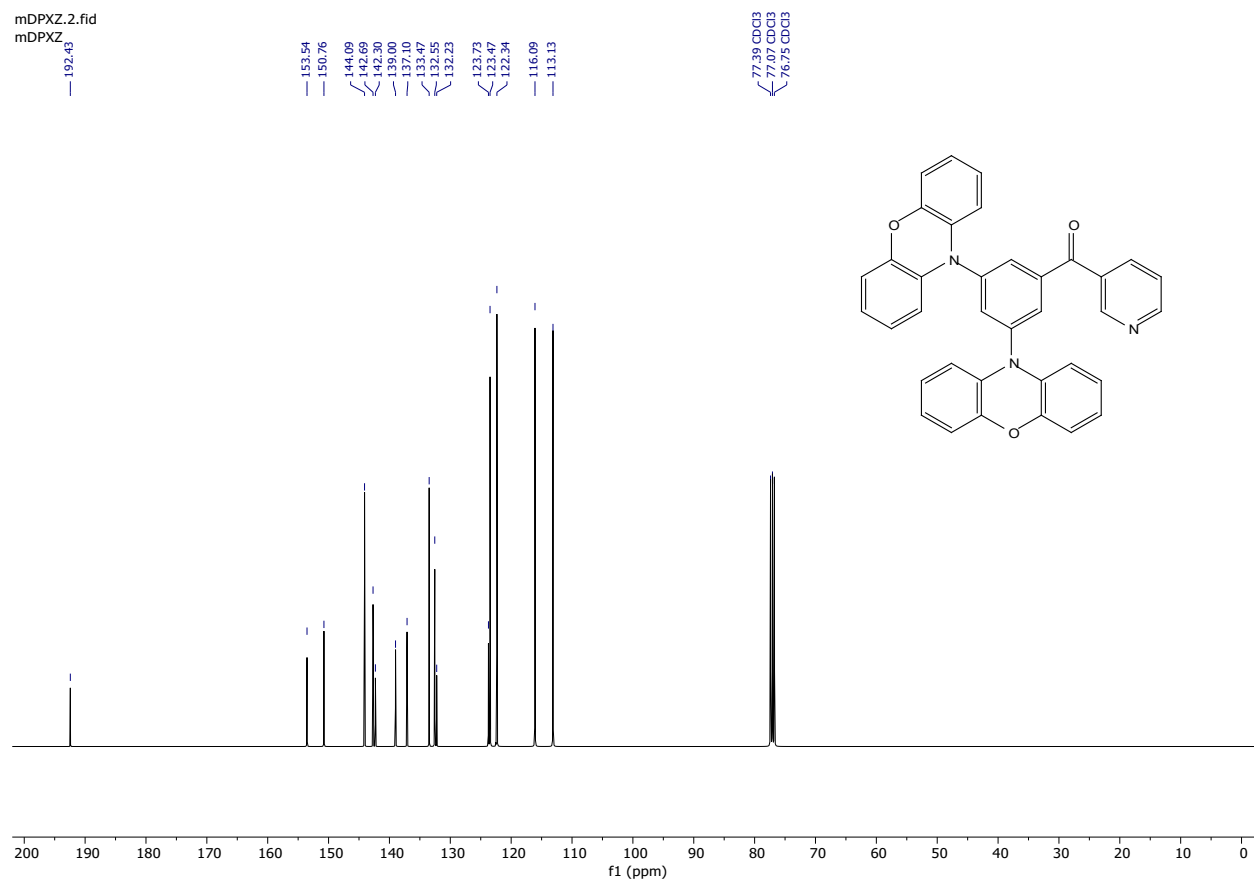


Figure S11. ^{13}C NMR of 3BPY-mDPXZ recorded in CDCl_3

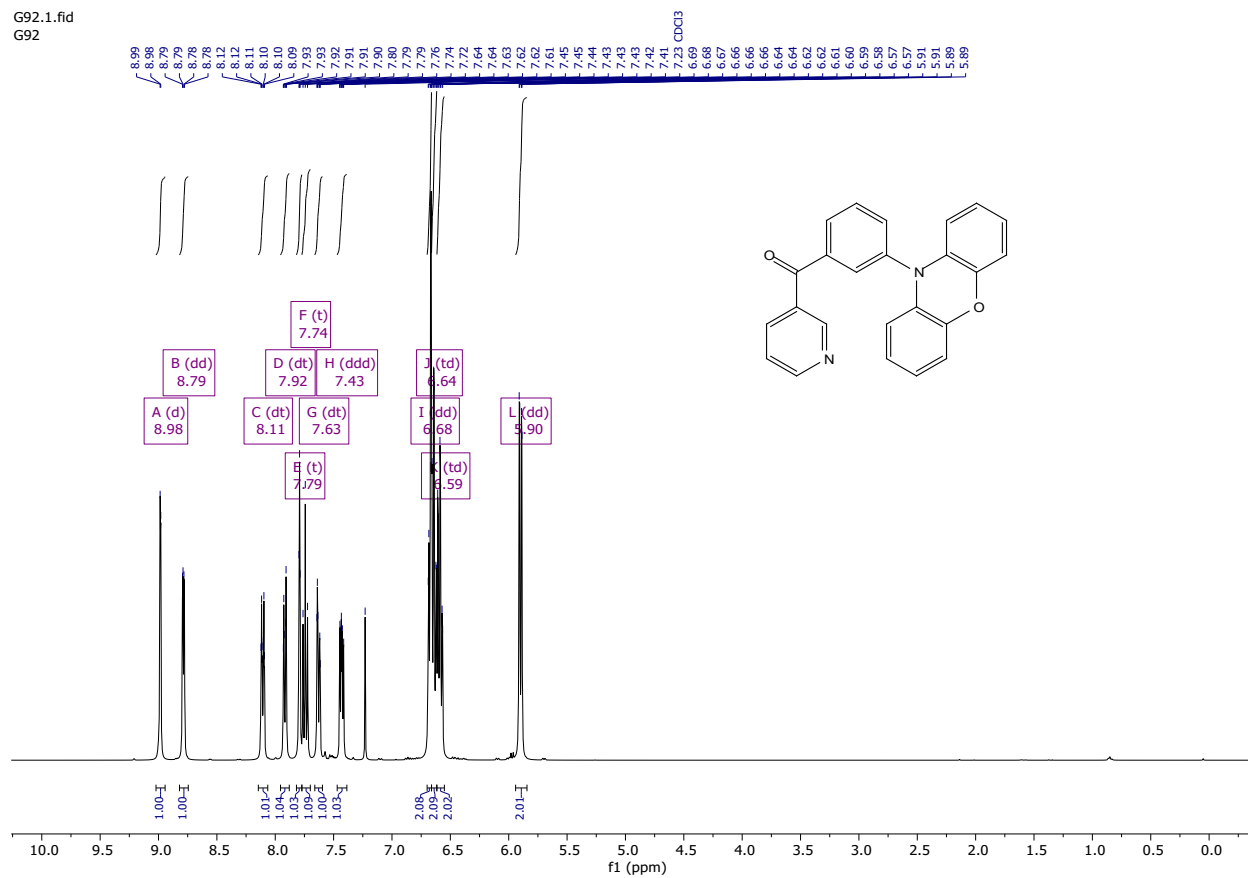


Figure S12. ^1H NMR of 3BP γ -mPXZ recorded in CDCl_3

G92.2.fid
G92

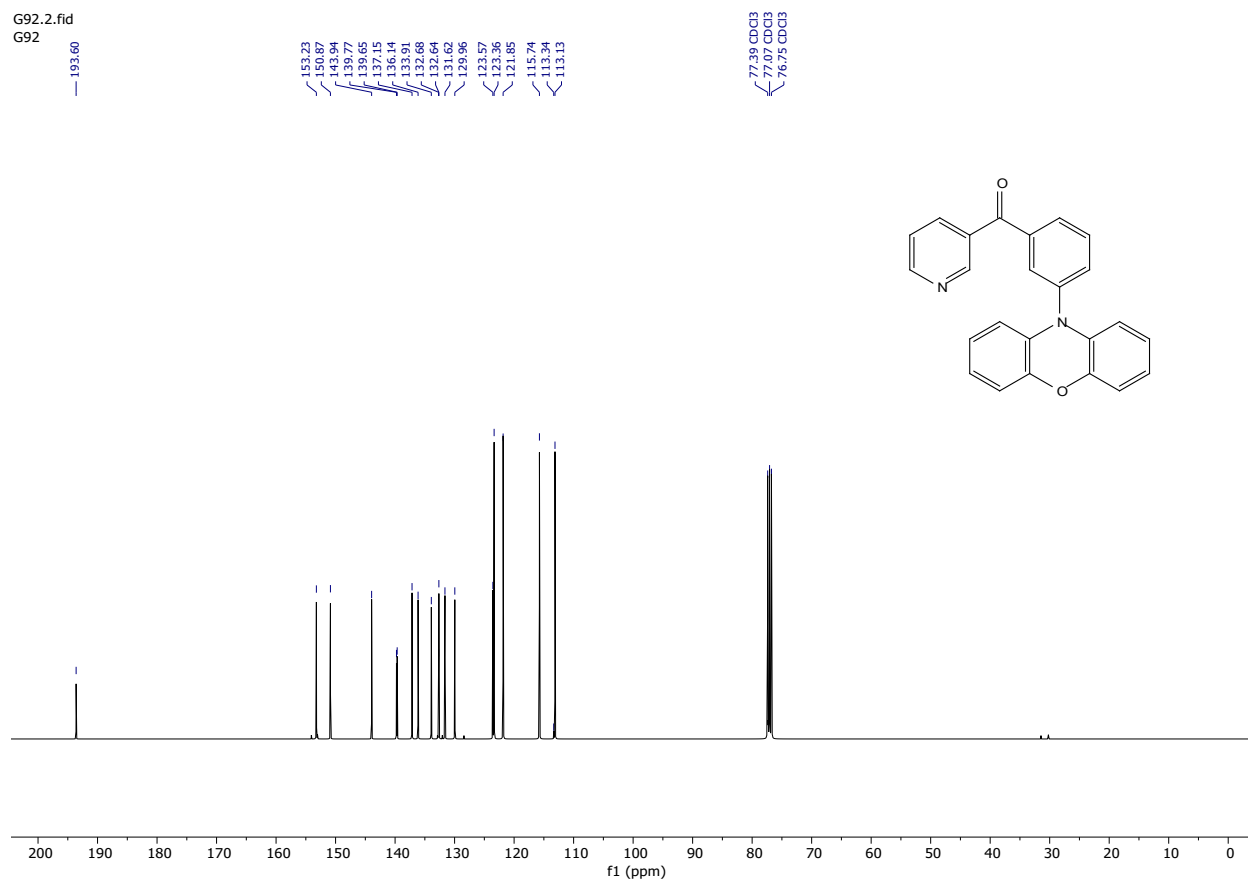


Figure S13. ^{13}C NMR of 3BPY-mPXZ recorded in CDCl_3

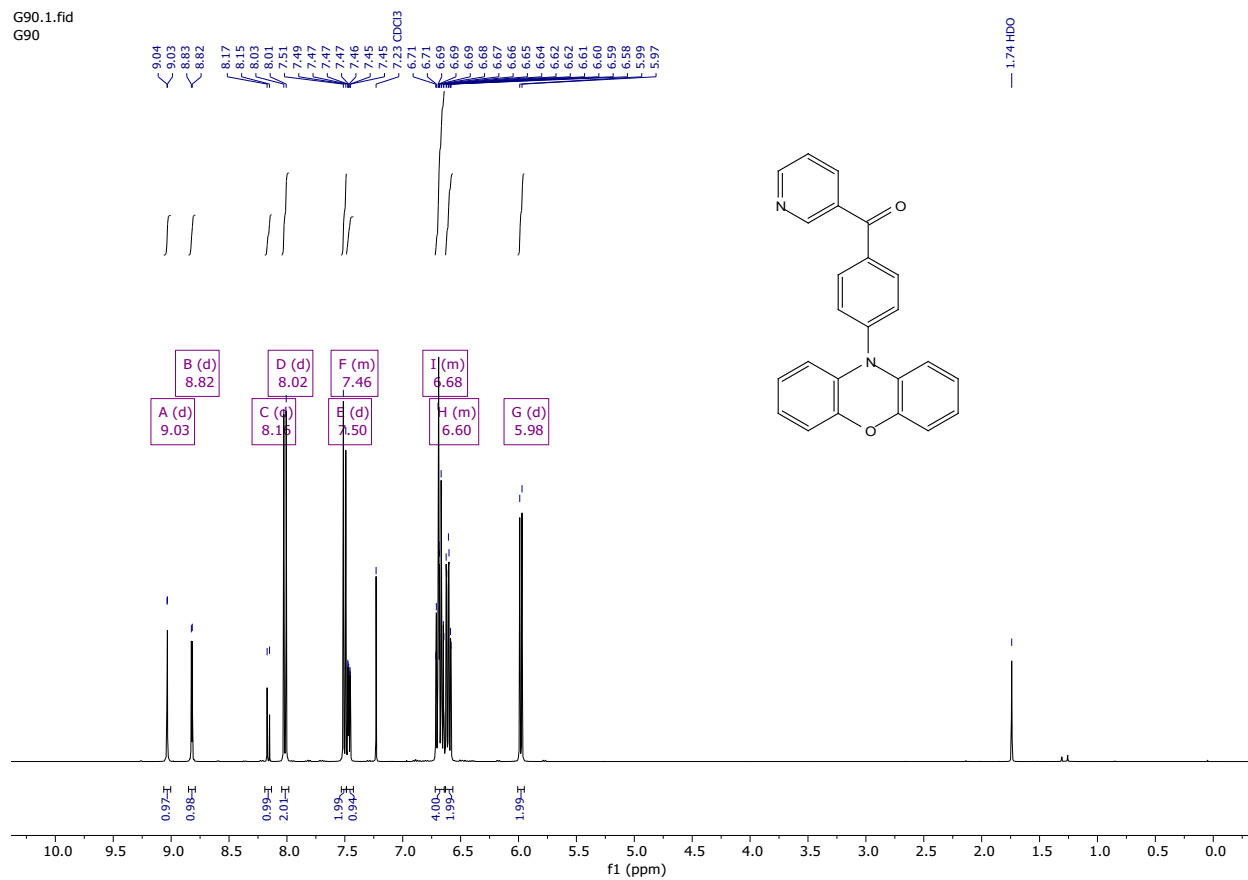


Figure S14. ¹H NMR of 3BPy-pPXZ recorded in CDCl₃

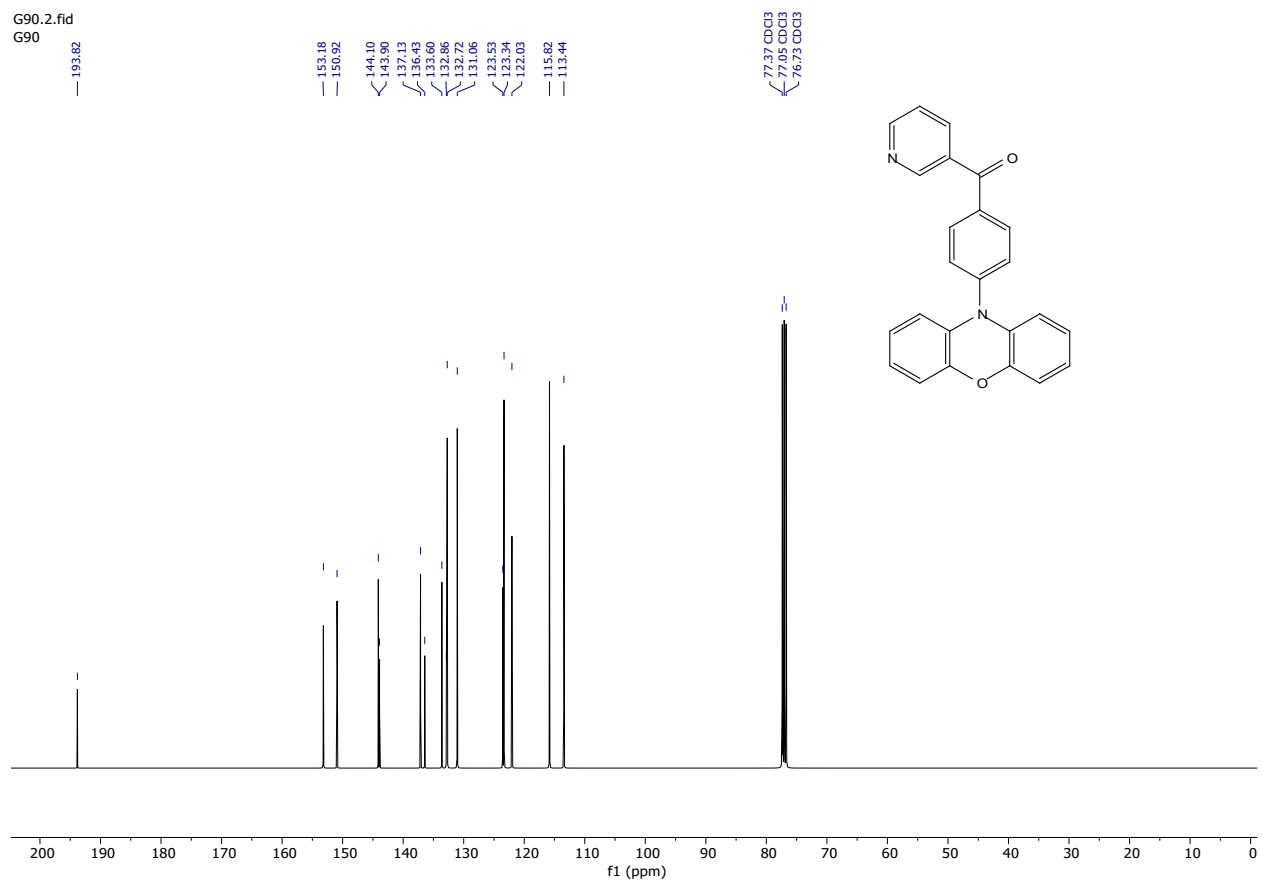


Figure S15. ^{13}C NMR of 3BPY-pPXZ recorded in CDCl_3

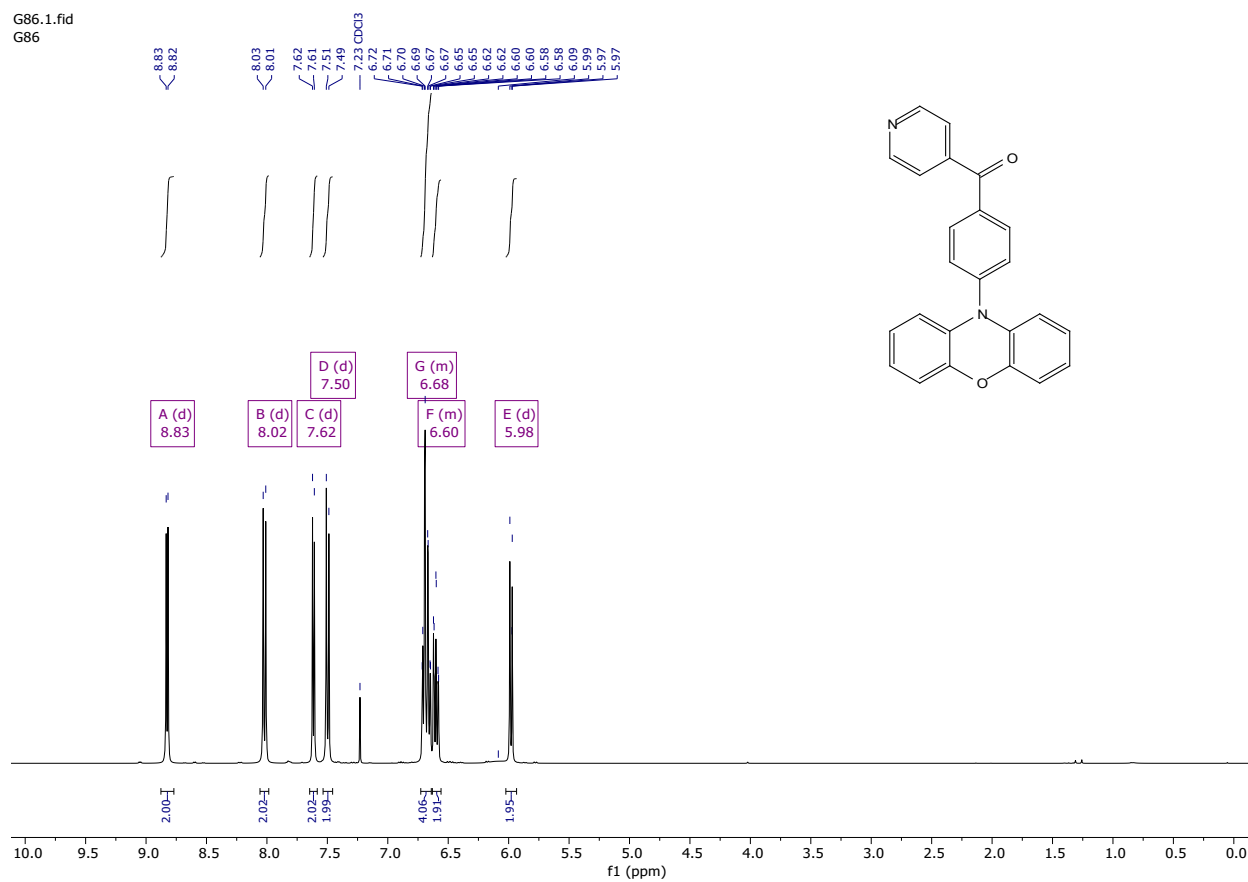


Figure S16. ¹H NMR of 4BPY-pPXZ recorded in CDCl₃

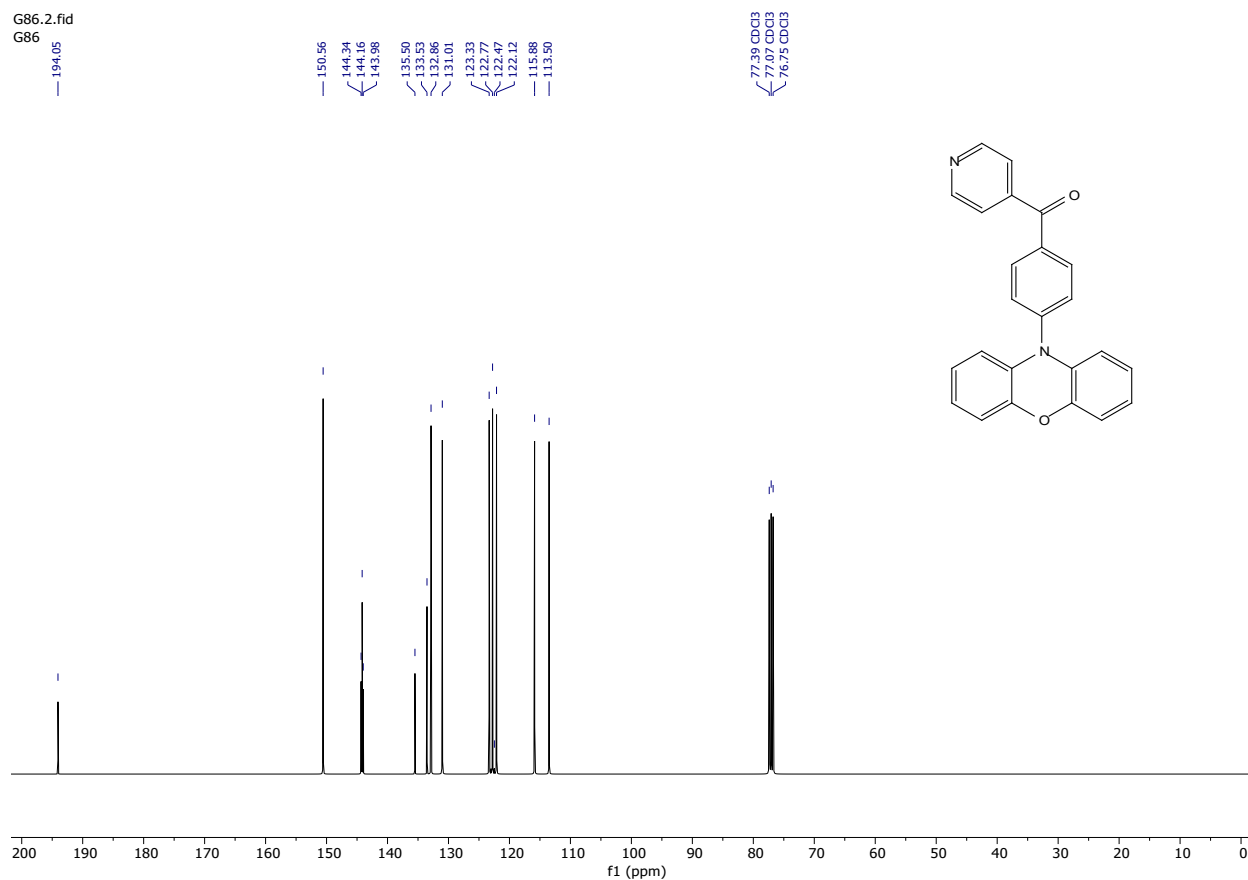


Figure S17. ^{13}C NMR of 4BPY-pPXZ recorded in CDCl_3

Reference

1. N. Yadav, U. Deori, E. Ravindran, B. Sk and P. Rajamalli, *Journal of Materials Chemistry C*, 2023, **11**, 16368-16376.
2. X. Zhou, Y. Xiang, F. Ni, Y. Zou, Z. Chen, X. Yin, G. Xie, S. Gong and C. Yang, *Dyes and Pigments*, 2020, **176**, 108179.
3. A. Shafiee, M. Mat Salleh and M. Yahaya, *Sains Malaysiana*, 2011, **40**, 173-176.
4. G. P. Nanda, R. Suraksha and P. Rajamalli, *ACS Materials Au*, 2024, DOI: 10.1021/acsmaterialsau.4c00036.
5. T. Matulaitis, P. Imbrasas, N. A. Kukhta, P. Baronas, T. Bučiūnas, D. Banevičius, K. Kazlauskas, J. V. Gražulevičius and S. Juršėnas, *The Journal of Physical Chemistry C*, 2017, **121**, 23618-23625.
6. U. Deori, N. Yadav, G. P. Nanda, K. L. Kumawat and P. Rajamalli, *ACS Applied Electronic Materials*, 2023, **5**, 4959-4967.
7. G. P. Nanda, B. Sk, N. Yadav, S. Rajamanickam, U. Deori, R. Mahashaya, E. Zysman-Colman and P. Rajamalli, *Chemical Communications*, 2021, **57**, 13728-13731.